molecules

MDPI

Article

Synthesis, Characterization, and Reactivity Studies of New Cyclam-Based Y(III) Complexes

Filipe Madeira [1], Luis F. Veiros [1], Luis G. Alves [2,*] and Ana M. Martins [1,*]

[1] Centro de Química Estrutural, Instituto Superior Técnico, Universidade de Lisboa, Av. Rovisco Pais 1, 1049-001 Lisbon, Portugal
[2] Centro de Química Estrutural, Associação do Instituto Superior Técnico para a Investigação e Desenvolvimento, Av. António José de Almeida nº 12, 1000-043 Lisbon, Portugal
* Correspondence: luis.g.alves@tecnico.ulisboa.pt (L.G.A.); ana.martins@tecnico.ulisboa.pt (A.M.M.)

Abstract: [(Bn_2Cyclam)Y($N(SiMe_3)_2$)] was prepared by reaction of H_2Bn_2Cyclam with $Y[N(SiMe_3)_2]_3$. The protonation of the macrocycle ligand in [(Bn_2Cyclam)Y($N(SiMe_3)_2$)] is observed upon reaction with $[HNMe_3][BPh_4]$ leading to the formation of [(HBn_2Cyclam)Y($N(SiMe_3)_2$)][BPh_4]. DFT analysis of [(Bn_2Cyclam)Y($N(SiMe_3)_2$)] showed that the HOMO is located on the anionic nitrogen atoms of the cyclam ring indicating that protonation follows orbital control. Addition of H_2Bn_2Cyclam and $H_2(^{3,5\text{-}tBu2}Bn)_2$Cyclam to a 1:3 mixture of YCl_3 and $LiCH_2SiMe_3$ in THF resulted in the formation of [(($C_6H_4CH_2$)BnCyclam)Y(THF)(μ-Cl)Li$(THF)_2$] and [Y{$(\eta^3\text{-}^{3,5\text{-}tBu2}Bn)_2$Cyclam}Li(THF)], respectively. The reaction of $H_2{}^{3,5\text{-}tBu2}Bn_2$Cyclam with $Y(CH_2SiMe_3)_3(THF)_2$ was studied and monitored by a temperature variation NMR experiment revealing the formation of [($^{3,5\text{-}tBu2}Bn_2$Cyclam)Y(CH_2SiMe_3)]. Preliminary catalytic assays have shown that [Y{$(\eta^3\text{-}^{3,5\text{-}tBu2}Bn)_2$Cyclam}Li(THF)] is a very efficient catalyst for the intramolecular hydroamination of 2,2-diphenyl-pent-4-enylamine.

Keywords: tetraazamacrocycles; cyclam ligands; Y(III) complexes; DFT calculations

Citation: Madeira, F.; Veiros, L.F.; Alves, L.G.; Martins, A.M. Synthesis, Characterization, and Reactivity Studies of New Cyclam-Based Y(III) Complexes. *Molecules* **2023**, *28*, 7998. https://doi.org/10.3390/molecules28247998

Academic Editors: Mário J. F. Calvete and Mariette M. Pereira

Received: 24 November 2023
Revised: 4 December 2023
Accepted: 5 December 2023
Published: 7 December 2023

1. Introduction

The research work in the field of rare-earth metals, which encompasses yttrium, has mostly been dominated by cyclopentadienyl complexes [1]. The post-metallocene technology in the chemistry of rare-earth metals has been growing at a fast pace to fulfill the requirements of more applicable and suitable catalysts. In this context, yttrium complexes have attracted much attention due to their high reactivity in intramolecular hydroamination [2–10] as well as olefin [11–14] and cyclic ester [15–20] polymerization catalysis. The hard Lewis acid nature of yttrium explains its tendency to coordinate to ligands that contain oxygen and nitrogen donors [21–28]. Although a rich chemistry of delocalized systems possessing aminato, guanidinato, and β-diketiminato ligands have emerged, chelating dianionic diamido ligands with located charges seemed to be depreciated and far from reaching those levels of importance. Nitrogen containing macrocycles, especially saturated azamacrocycles with diamido functions, became powerful ligands to stabilize rare-earth and early transition metals. The dianionic cyclen derivative 1,7-Me_2TACD (TACD = 1,4,7,10-tetraazacyclododecane) was used as a surrogate for the bis(cyclopentadienyl) scaffold to prepare Y [29], Sc [30], and Zr [31] alkyl and hydrido species. The reaction of $Y(\eta^3\text{-}C_3H_5)_3$(1,4-dioxane) with H_2(1,7-Me_2TACD) afforded the dimeric allyl complex $[Y(\eta^3\text{-}C_3H_5)$(1,7-Me_2TACD)$]_2$. Treatment of $[Y(\eta^3\text{-}C_3H_5)$(1,7-Me_2TACD)$]_2$ with two equiv. of KC_3H_5 gave the heterometallic potassium yttrium allyl complex $[Y((\eta^3\text{-}C_3H_5)_2)$(1,7-$Me_2$TACD)K$(THF)]_n$, which originated the hydride cluster complex [(Y(1,7-Me_2TACD))$(\mu_3\text{-}H)_2$(Y(1,7-Me_2TACD))$(\mu_2\text{-}H)_2$(Y(1,7-Me_2TACD))$(\mu_3\text{-}H)_2$(Y(1,7-Me_2TACD)$K_2(THF)_4$] upon hydrogenolysis with 1 bar of molecular hydrogen in THF [29].

In our group, the chemistry of Zr(IV) complexes supported by *trans*-disubstituted cyclams has been extensively studied [32–40]. Attempting to further explore the use

of cyclam derivatives as ancillary ligands for early transition metals, we describe here the synthesis, characterization, and reactivity of the first Y(III) complexes supported by dianionic diamino-diamine cyclams.

2. Results and Discussion

Treatment of the commercially available $Y[N(SiMe_3)_2]_3$ with $H_2Bn_2Cyclam$, **1**, in THF, gave the yttrium amido derivative $[(Bn_2Cyclam)Y(N(SiMe_3)_2)]$, **2**, as Scheme 1 shows.

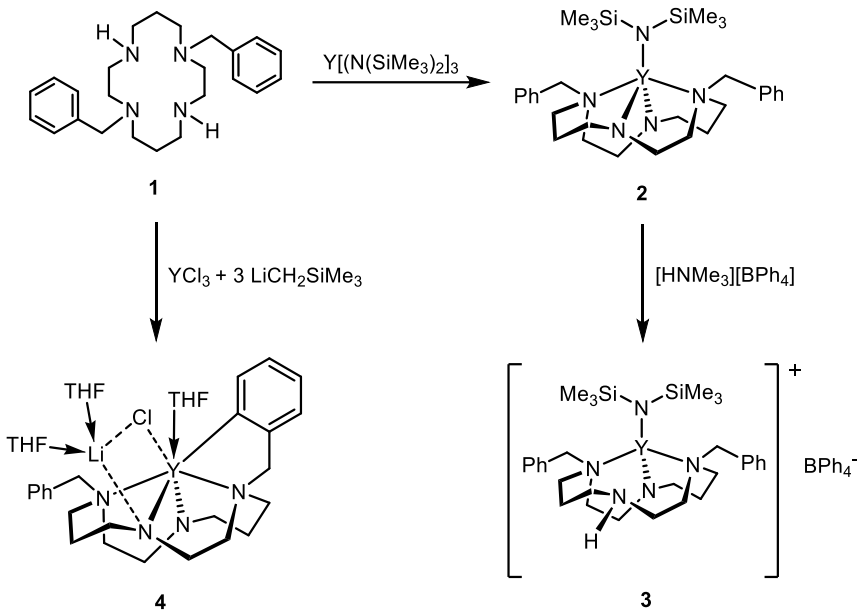

Scheme 1. Synthetic route for the preparation of complexes **2**–**4**.

Crystals of **2** suitable for single-crystal X-ray diffraction were obtained from a THF solution at −20 °C. Figure 1 shows a depiction of the solid-state molecular structure of **2**.

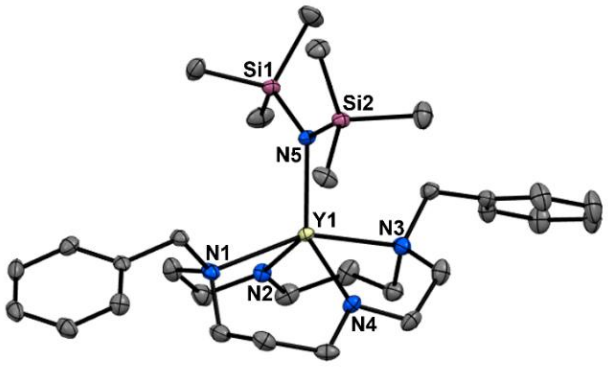

Figure 1. ORTEP diagram of $[(Bn_2Cyclam)Y(N(SiMe_3)_2)]$, **2**, using 40% probability level ellipsoids. Hydrogen atoms were omitted for clarity. Selected bond lengths (Å) and angles (°): Y(1)–N(1) 2.479(3), Y(1)–N(2) 2.226(3), Y(1)–N(3) 2.482(2), Y(1)–N(4) 2.214(2), Y(1)–N(5) 2.303(2); N(2)–Y(1)–N(4) 109.69(9), N(2)–Y(1)–N(5) 128.56(9), N(4)–Y(1)–N(5) 121.74(9), N(1)–Y(1)–N(3) 152.85(8).

The yttrium is coordinated to the four nitrogen atoms of the macrocycle and to one bis(trimethylsilyl)amido ligand in a distorted trigonal bipyramid geometry, with the equatorial plane defined by atoms N(2), N(4), and N(5). The axial positions are occupied by N(1) and N(3) atoms of the macrocycle. The value of $\tau = 0.72$ for the yttrium center attests to the high distortion observed in the solid state because the atoms of the axial positions, which are enclosed in the macrocycle, are subjected to structural constraints. In solution, the mobility of the macrocycle is enhanced, and average positions of N(1) and N(3) are the

symmetrical axial positions. Nevertheless, the τ value is closer to 1 than 0 and the best description for the structure is trigonal bipyramidal [41]. The metal is located within the equatorial plane, where the sum of N(2)–Y(1)–N(4), N(2)–Y(1)–N(5) and N(4)–Y(1)–N(5) angles is 360° as expected. The dihedral angles N–C–C–N that characterize the five-membered rings are negative (−47.1(4)° and −46.4(4)°). The sum of angles around the N_{amido} groups of the macrocycle is approximately 356°, which corroborates with sp^2 hybridization for the nitrogen atoms and is consistent with a Y–N multiple bond. The Y–N_{amido} (2.226(3) Å and 2.214(2) Å) and Y–N_{amine} (2.479(3) Å and 2.482(2) Å) bond lengths to the macrocyclic ligand are within the range observed for pentacoordinated Y complexes [42–44]. The Y–$N(SiMe_3)_2$ distance of 2.303(2) Å is slightly longer than the ones between yttrium and the N_{amido} atoms of the macrocycle but in agreement with values reported in the literature [43–48].

The ^1H and $^{13}C\{^1H\}$ NMR spectra of **2**, as Figure S1 depicts (Supplementary Materials), show C_2 symmetry in solution. Multiple resonances are identified in the ^1H NMR integrating overall to twenty protons and corresponding to the H_{anti} and H_{syn} protons of the macrocyclic backbone. The AB spin system assigned for the benzyl protons is positioned at low field with $^2J_{H\text{-}H}$ = 15 Hz. In the $^{13}C\{^1H\}$ NMR spectrum, one set of signals for the aromatic carbons is observed as well as six signals for the methylene carbons of the ancillary macrocycle ligand. Interestingly, a long-range virtual Y–C coupling in the two carbon signals assigned for the [C2] chain with a $^2J_{Y\text{-}C}$ = 2 Hz is observed. This value is within the expected range, but it is smaller than others reported (~3–5 Hz) [49,50], possibly because a nitrogen atom is positioned between the Y and C atoms.

In order to acquire more details regarding the nature of the yttrium-nitrogen bonds in complex **2**, DFT calculations were carried out at the M06/6-31G** level. In the geometry optimized for **2**, the Y–N_{amido} bond lengths (2.22 Å and 2.27 Å, Figure 2) are shorter and stronger (Wiberg indices of 0.40–0.41) than the Y–N_{amine} bond lengths (2.49 Å and WI of 0.12). The atomic charges (C) calculated by means of a Natural Population Analysis (NPA) [51–56] for the nitrogen atoms in **2** (Figure 2) show that the N_{amido} atom (C_{N5} = −1.81) of the $N(SiMe_3)_2$ ligand is remarkably more negative than the N_{amido} atoms within the macrocycle (C_{N2} = C_{N4} = −0.98). The N_{amine} atoms of the neutral amine functions are less negative with charge values of C_{N1} = C_{N3} = −0.62.

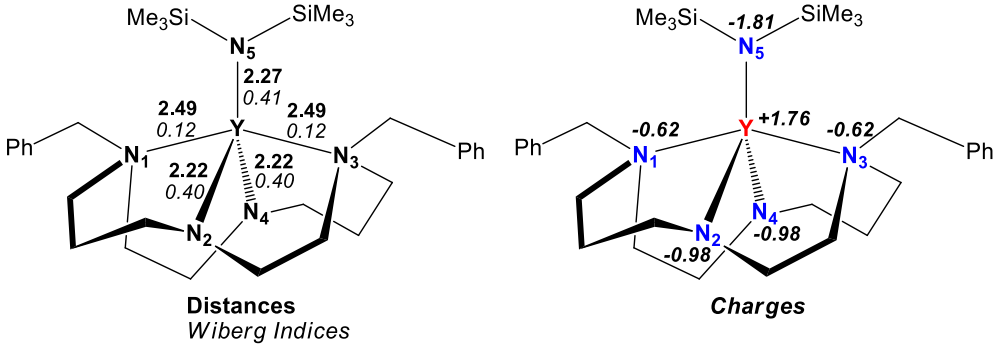

Figure 2. Molecular structures of **2** with the more relevant distances (Å, in bold) and Wiberg indices (in italics) indicated on the left and the atomic charges calculated for Y and N atoms indicated on the right.

Figure 3 illustrates representations of the HOMO and HOMO–1 of complex **2**. Both orbitals are mainly located at the N_{amido} atoms of the macrocyclic ligand and correspond essentially to the anti-symmetric and the symmetric combinations of the N_{amido} lone pairs, respectively.

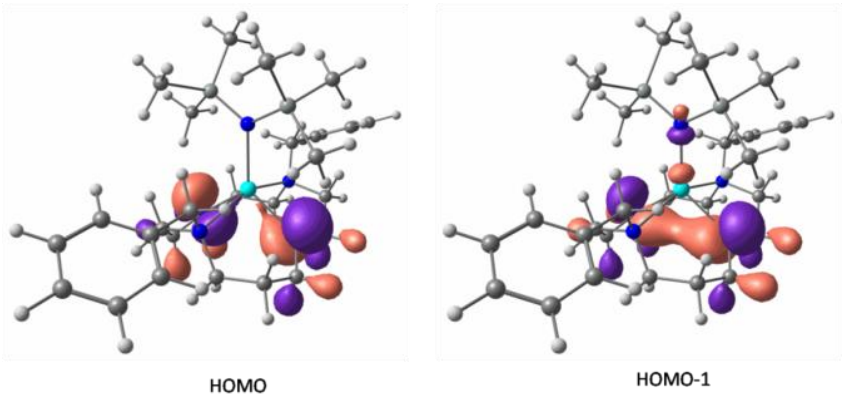

Figure 3. Representations of the HOMO and HOMO–1 of complex [(Bn_2Cyclam)Y($N(SiMe_3)_2$)], **2**.

The reaction of **2** with [$HNMe_3$][BPh_4] in THF gave the cationic complex [(HBn_2Cyclam) Y($N(SiMe_3)_2$)][BPh_4] (**3**, Scheme 1) that was isolated as a white solid almost quantitatively. This reaction shows that protonation is selective and occurs in the N_{amido} of the cyclam-based ligand. Thus, the acidic proton was transferred to one of the N_{amido} atoms where the HOMO is centered instead of interacting with the most negatively charged nitrogen atom located in the $N(SiMe_3)_2$ group. This result indicates that the reaction follows an orbital control.

Crystals of **3** suitable for single-crystal X-ray diffraction were obtained from a concentrated solution of THF double-layered with toluene at −20 °C. Figure 4 shows a depiction of the solid-state molecular structure of **3**.

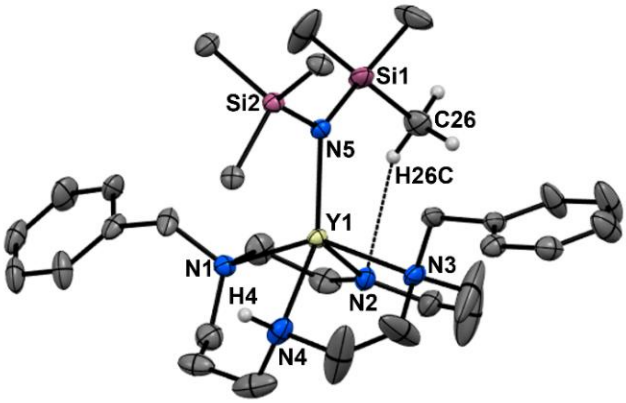

Figure 4. ORTEP diagram of [(HBn_2Cyclam)Y($N(SiMe_3)_2$)][BPh_4], **3**, using 30% probability level ellipsoids. The tetraphenylborate anion was omitted for clarity. Hydrogen bonds are indicated by dashed lines. Selected bond lengths (Å) and angles (°): Y(1)–N(1) 2.449(3), Y(1)–N(2) 2.141(3), Y(1)–N(3) 2.451(3), Y(1)–N(4) 2.473(4), Y(1)–N(5) 2.233(3); N(2)–Y(1)–N(4) 107.3(1), N(2)–Y(1)–N(5) 113.6(1), N(4)–Y(1)–N(5) 139.0(1), N(1)–Y(1)–N(3) 148.4(1).

The yttrium is bonded to the four nitrogen atoms enclosed within the macrocycle (three amines and one amido group) and to the nitrogen of the $N(SiMe_3)_2$ moiety, adopting a highly distorted trigonal bipyramidal geometry (τ = 0.68) [41]. The Y–N_{amine} and Y–N_{amido} bond lengths compare well with the ones reported to pentacoordinated yttrium complexes [42–44]. In comparison with complex **2**, there is a shortening of the Y–N_{amido} bond distances that corresponds to a decrease from 2.226(3) Å to 2.141(3) Å and from 2.303(2) Å to 2.233(3) Å in the Y(1)–N(2) and Y(1)–N(5) bond lengths, respectively. This difference results from the increase in the Lewis acidity of the metal due to the protonation of N(4) leading to C_1 symmetry for complex **3**. The change in the anionic amido group to a neutral amine affects the electron density in the metal center, which becomes more electropositive due to the cationic nature of the complex. The geometry around the yttrium reflects the modification occurring upon protonation. The enlargement of the N(4)–Y(1)–N(5) angle from 128.56(9)°

to 139.0(1)° and the reduction of the N(2)–Y(1)–N(5) angle from 121.74(9)° to 113.6(1)° are in the base of the high distortion observed for the geometry of **3**, where the $N(SiMe_3)_2$ ligand tilts towards the N(2) amido site. Moreover, the Si(2) atom is closer to yttrium than Si(1), which generates a high range Y···Si contact (Y(1)–Si(2) distance of 3.221(1) Å) that causes a virtual octahedral distortion. Rare cases of Y···Si interactions were observed, being relevant to the case of a diimine bis(phenolate) yttrium compound that exhibits an agnostic interaction between Y and Si atoms with a distance of 3.1583(9) Å [57]. The presence of the hydrogen bond interaction established between the N(2) and H(26c) atom with a distance of 2.703(3) Å strongly contributes to the tilting of the $N(SiMe_3)_2$ moiety. The sum of angles around N(2) and N(5) atoms are 359° and 360°, respectively, which is in agreement with the sp^2 hybridization for these nitrogen atoms, and thus, the N(2)···H(26c) interaction does not affect significantly the sp^2 character of N(2). The dihedral angles N–C–C–N that characterize the five-membered rings take values with different signals (−42.1(5)° for N(1)–C(1)–C(2)–N(2) and 10.0(18)° for N(3)–C(6)–C(7)–N(4)) because the nitrogen atoms are chiral due to the loss of symmetry of **3** and the two [C2] chains present different conformations [58]. The interaction of the cyclam ring with the $[BPh_4]$ anion is achieved by a N–H···π interaction characterized by a *d*(N(4)-centroid) value of 3.747 Å (see Figure S2) [59].

The NMR data of **3** are consistent with C_1 symmetry in solution. The ^{1}H NMR spectrum (see Figure S3) features twenty resonances assigned for the twenty methylene protons of the macrocycle, which correspond to ten signals in the $^{13}C\{^1H\}$ NMR spectrum (Figure S3). Two AB spin systems at 4.43 and 3.82 ppm ($^2J_{H\text{-}H}$ = 14 Hz) and 4.17 and 4.11 ppm ($^2J_{H\text{-}H}$ = 14 Hz) are attributed to the non-equivalent benzyl protons of the pending arms. The values of the coupling constants are in the range found for benzyl protons in yttrium diamine bis(phenolate) complexes [60,61]. The NH proton is not detectable in the ^{1}H NMR spectrum owing to the high overlapping of signals. The ^{11}B NMR spectrum displays a sharp signal at −6.5 ppm for the borate anion.

The reaction of H_2Bn_2Cyclam, **1**, with $Y(CH_2SiMe_3)_3(THF)_2$, prepared in situ from YCl_3 and $LiCH_2SiMe_3$ in a 1:3 ratio, in THF resulted in a complex mixture of species. Independent of the temperature, from −60 °C to room temperature, and the degree of dilution, it was not possible to isolate or identify the compounds present in solution. A few crystals that could be characterized by single-crystal X-ray diffraction correspond to $[((C_6H_4CH_2)BnCyclam)Y(THF)(\mu\text{-}Cl)Li(THF)_2]$, **4**, as Figure 5 shows. The molecular structure of **4** revealed that the macrocyclic ligand coordinated to yttrium is formally trianionic, formed by deprotonation of the two macrocycle secondary amines and *ortho* C-H activation of one benzyl substituent. It is likely that $[(Bn_2Cyclam)Y(CH_2SiMe_3)]$ is an intermediate of the reaction that develops to **4** by *ortho*-metalation of one benzyl group. This type of reaction was already observed in cyclam-based zirconium complexes $[(Bn_2Cyclam)ZrMe_2]$ and $[(Bn_2Cyclam)Zr(^nBu)_2]$, which eliminate methane and butane, respectively, to give $[((C_6H_4CH_2)_2Cyclam)Zr]$ [36]. Thus, it is not surprising that yttrium complexes, which readily promote C-H activation reactions, originate *ortho*-metalated species [62]. The molecular structure of **4** also reveals that the *ortho*-metalated intermediate may be stabilized by one equivalent of LiCl, a co-product of the synthesis of $Y(CH_2SiMe_3)_3(THF)_2$. The coordination of Cl^- to yttrium generates an -ate complex in which charge is balanced by Li^+ that binds to one macrocycle amido group. This interaction, which removes part of the electron density from yttrium to lithium, is reminiscent of the protonation reaction that led to complex **3**. The driving force for the reaction may be the strong ionic character of Y(III) and its tendency to form charge-separated species, either zwitterions or ions pairs, often observed for amido yttrium complexes in polar solvents [63,64].

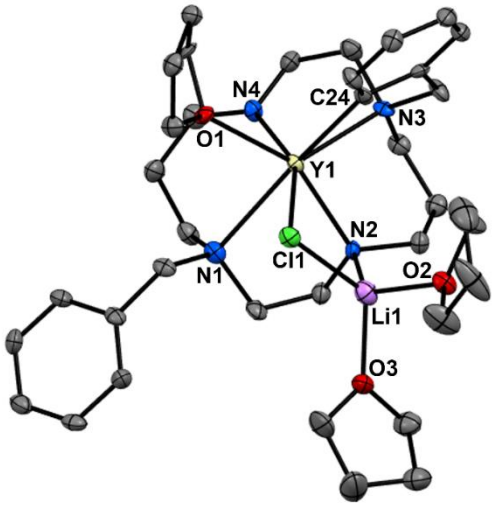

Figure 5. ORTEP diagram of [((C$_6$H$_4$CH$_2$)BnCyclam)Y(THF)(μ-Cl)Li(THF)$_2$], **4**, using 40% probability level ellipsoids. Co-crystallized THF molecule and hydrogen atoms were omitted for clarity. Selected bond lengths (Å) and angles (°): Y(1)–N(1) 2.676(4), Y(1)–N(2) 2.311(4), Y(1)–N(3) 2.562(3), Y(1)–N(4) 2.273(4), Y(1)–Cl(1) 2.825(1), Y(1)–O(1) 2.492(3), Y(1)–C(24) 2.479(5); N(1)–Y(1)–N(2) 71.6(1), N(2)–Y(1)–N(3) 79.8(1), N(3)–Y(1)–N(4) 70.7(1), N(4)-Y(1)-N(1) 81.9(1), C(24)–Y(1)–Cl(1) 82.5(1).

The yttrium is heptacoordinated in a distorted capped trigonal prismatic geometry. The four nitrogen atoms of the macrocycle occupy the equatorial plane, C(24) and Cl(1) occupy the axial positions, and the trigonal prism is capped by O(1). The yttrium atom lies 1.205(2) Å above the average plane defined by the four nitrogen atoms of the macrocycle that deviate between 0.079(2) Å and 0.085(2) Å from the plane. The asymmetry of the molecule is reflected in the distances between the yttrium and the nitrogen atoms. The Y–N$_{amido}$ distances of 2.311(4) Å and 2.273(4) Å are within the range of values previously reported for yttrium complexes. However, the Y(1)–N(2) distance is longer than Y(1)–N(4), in agreement with the bridging location of N(2) between yttrium and lithium. Y–N$_{amine}$ distances of 2.676(4) Å and 2.562(3) Å are considerably longer than the ones previously observed for **2** and **3**, despite the value of 2.562(3) Å found for Y(1)–N(3) which compares well with Y–N$_{amine}$ distances of 2.527(3) Å and 2.568(2) Å in [Y(2,6-Et$_2$C$_6$H$_3$NCH$_2$CH$_2$)$_2$NMe)(o-C$_6$H$_4$CH$_2$NMe$_2$)] [65] and [Y(Me$_2$NCH$_2$CH$_2$-(CH$_2$-2-O-3,5-C$_6$H$_2$^{t}Bu$_2$)$_2$)(C$_6$H$_4$CH$_2$NMe$_2$)] [66], respectively. The longer Y–N$_{amine}$ distance at 2.676(4) Å reflects the high coordination number of yttrium and possibly the geometry distortion caused by THF and the bridging Y–Cl–Li arrangement. The Y(1)–Cl(1) bond length at 2.825(1) Å is much longer than the Y–Cl bond lengths found in neutral yttrium complexes (2.618(4) Å) [61,66,67] due to the bridging nature of the chlorido ligand connecting both Y and Li centers. The Li(1)–Cl(1) distance is 2.33(1) Å, which corresponds essentially to the sum of the ionic radii of Li^+ (0.76 Å) and Cl^- (1.84 Å) [68,69]. For comparison, Y–Cl distances in [(DAB)Y(THF)$_2$(μ-Cl)$_2$Li(THF)$_2$], DAB = (2,6-C$_6$H$_3$^{i}Pr$_2$)NC(Me)=C(Me)N(2,6-C$_6$H$_3$^{i}Pr$_2$)) are 2.716(1) Å and correspond to the longest described in the literature [70]. The Y(1)–O(1) and Y(1)-C(24) distances of 2.492(3) and 2.479(5) Å, respectively, are within the usual ranges [66,71–73]. The lithium cation displays typical tetrahedral coordination with regular Li–N and Li–O distances [44,74,75].

It was previously reported that 3,5-disubstitution of the benzyl pending arms of cyclam by bulky groups made C-H activation reactions difficult to occur [76]. This feature might allow the stabilization of yttrium alkyl complexes having dianionic cyclams as anchoring ligands. Thus, the reaction of H$_2$($^{3,5\text{-}t\text{Bu}2}$Bn)$_2$Cyclam, **5**, with Y(CH$_2$SiMe$_3$)$_3(THF)_2$, prepared in situ from YCl$_3$ and LiCH$_2$SiMe$_3$ in a 1:3 ratio, in THF at −20 °C was attempted. The resulting compound was the yttrium ate complex [Y{(η^3-$^{3,5\text{-}t\text{Bu}2}$Bn)$_2$Cyclam}Li(THF)], **6**, which was obtained in 26% yield. This complex is the product that would be expected from the reaction of [Li(THF)$_4$][Y(CH$_2$SiMe$_3$)$_4$] with **5**. Although the formation of the

product is not consistent with the stoichiometry of the reagents, it might be possible that the reaction of YCl_3 and 3 equiv. of $LiCH_2SiMe_3$ in THF would give rise to a mixture where, in addition to $Y(CH_2SiMe_3)_3(THF)_2$, other compounds might be present. This assumption is in accordance with the occurrence of equilibria between mono-, di-, tri-, and tetraalkyl yttrium species formed by σ-bond metathesis reactions [77–79]. In view of this result, we tentatively suggest that the formation of **6** may involve the intermediate formation of $Li[\{(^{3,5\text{-}tBu2}Bn_2)_2Cyclam\}Y(CH_2SiMe_3)_2]$ that, upon C-H activation of the methylene protons of the benzyl groups would generate tetramethylsilane and **6** where the cyclam pending arms show η^3-benzallyl coordination to yttrium (see Scheme 2).

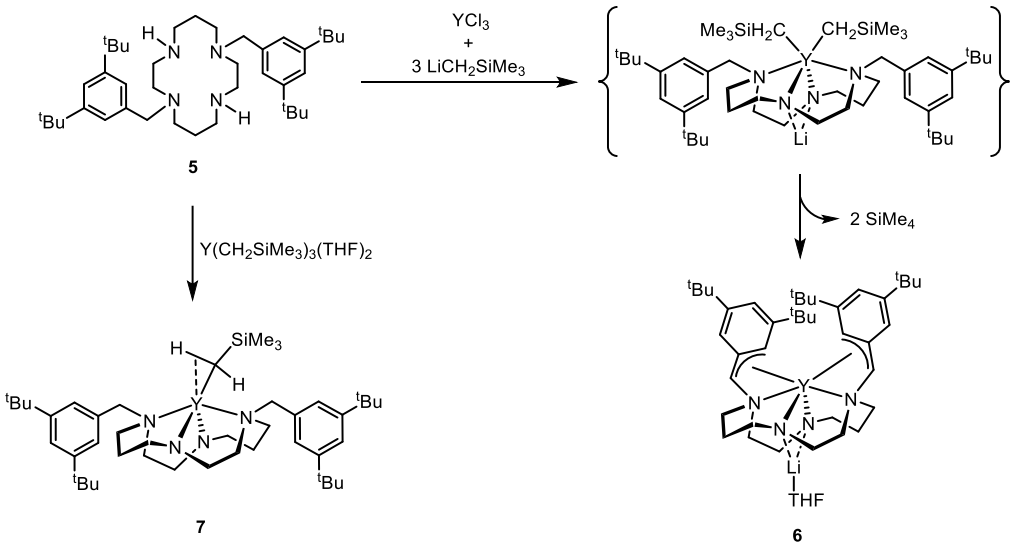

Scheme 2. Synthetic route for the preparation of complexes **6** and **7**.

Considering the structure of complex **4**, where the yttrium mono-*ortho*-metalated cyclam complex is stabilized by LiCl, it is conceivable that species like $[R_2Y(N\text{-}Cyclam\text{-}NLi)]$ are intermediates in reactions of yttrium complexes and lithium cyclams. The ^1H NMR spectrum of **6**, as Figure S4 depicts, is consistent with a C_2-symmetric species. Ten resonances, integrating to two protons each, assigned to the macrocyclic methylene protons are observed between 4.2 and 1.5 ppm. The η^3-benzyl groups give rise to a characteristic set of four resonances at 6.56 ppm (Ar-H_{allyl}), 6.15 ppm (Ar-H_{para}), 4.77 ppm (Ar-*H*), and 3.67 ppm (NC*H*Ar), which integrate eight protons and the ^{t}Bu substituents give rise to two resonances at 1.57 and 1.39 ppm that integrate eighteen protons each. THF resonances are broad but integrate one molecule per macrocycle. The η^3-benzyl arms give rise to diagnostic C-H carbon signals in the $^{13}C\{^1H\}$ NMR spectrum (Figure S5), which appear at 113.9 ppm (*Ar*-H_{allyl}), 105.3 ppm (*Ar*-H_{para}), 90.5 ppm (*Ar*-H), and 76.3 ppm (NCHAr). The carbon signal assigned for the NCHAr function exhibits a Y–C coupling constant of $^2J_{Y\text{-}C}$ = 3.0 Hz [49].

Crystals of $[Y\{(\eta^3\text{-}^{3,5\text{-}tBu2}Bn)_2Cyclam\}Li(THF)]$, **6**, suitable for single-crystal X-ray diffraction were obtained from a THF solution at −20 °C. Figure 6 shows the solid-state molecular structure of **6**.

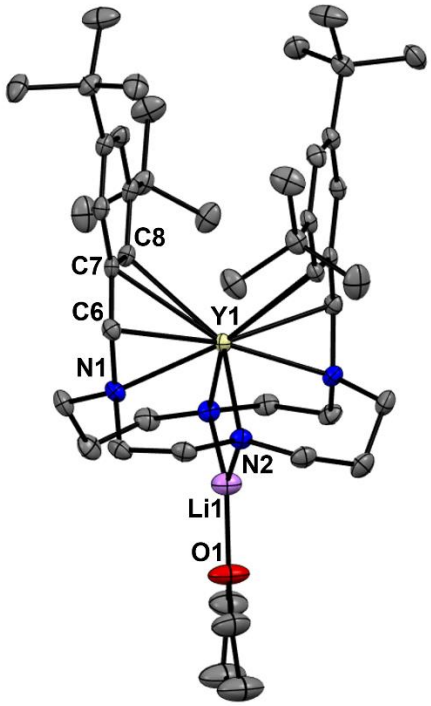

Figure 6. ORTEP diagram of [Y{(η^3-$^{3,5\text{-}tBu2}$Bn)$_2$Cyclam}Li(THF)], **6**, using 40% probability level ellipsoids. Hydrogen atoms were omitted for clarity. Half molecule is generated by the symmetry operation −x + 1, y, −z + 3/2. Selected bond lengths (Å) and angles (°): Y(1)–N(1) 2.403(2), Y(1)–N(2) 2.316(2), Y(1)–C(6) 2.536(2), Y(1)–C(7) 2.754(2), Y(1)–C(8) 2.746(2), Li(1)–N(2) 1.998(3), Li(1)–O(1) 1.851(5); N(2)–Y(1)–N(2$_1) 87.3(8), C(7)–Y(1)–C(7$_1) 106.5(8), N(2)–Li(1)–N(2$_1) 106.3(2), N(2)–Li(1)–O(1) 126.9(1).

The compound crystallized in the monoclinic system, *I*2/c space group with half molecule of **6**, and THF in the asymmetric unit. The geometry around the yttrium atom is best described as distorted bicapped tetrahedron, considering Y(1)–C(7) as the average bond of the η^3-benzallyl system (see Figure S6). The tetrahedron is defined by the atoms N(2), N(2$_1), C(7), and C(7$_1) and it is capped by the N(1) and N(1$_1) atoms. The lithium atom adopts a distorted trigonal geometry. The Y–N_{amine} and Y–N_{amido} distances of 2.403(2) Å and 2.316(2) Å, respectively, are comparable with the values observed for complexes **2**, **3**, and **4**. The sum of angles around N(2) is 346.6° and agrees with its pyramidalization due to the bridging coordination between yttrium and lithium. The Y–C bond distances of the η^3-benzallyl system fall in the range of 2.536(2) to 2.754(2) Å and compare well with Y–C bond distances reported for [Y(η^3-$C_6H_5CHNMe_2)_3$] [80]. The C(6)–C(7) and C(7)–C(8) bond lengths of 1.405(3) Å and 1.430(3) Å, respectively, disclose essentially symmetric bonds that correspond to a delocalized allyl system, η^3-coordinated to yttrium. The bonding of N_{amido} atoms to Li causes the N(2)–Y(1)–N(2$_1) angle to be shortened (87.3(8)°) in comparison to the typical 109.5° of a regular tetrahedron. Interestingly, the O(1)–Li(1)–Y(1) angle of 180.0° points out that O(1), Li(1), and Y(1) atoms are collinear. In addition, Y(1), N(2), Li(1), N(2$_1), and O(1) are also co-planar and define the symmetry plane in **6**.

To shed some light on the subject, the reaction between **5** and Y($CH_2SiMe_3)_3(THF)_2$ was monitored by a variation temperature ^{1}H NMR experiment. Figure S7 displays the spectra which show that the resonances corresponding to the macrocycle and the CH_2SiMe_3 ligand bonded to yttrium start to resolve above −40 °C. At −30 °C, one set of resonances attributed to a C_2-symmetric species that is assigned as [{($^{3,5\text{-}tBu2}$Bn)$_2$Cyclam}Y(CH_2SiMe_3)], **7**, is clearly observed (see Scheme 2). The ^{1}H NMR spectrum at −30 °C (Figure S8) presents the assignment of the main resonances of **7**. The methylene protons of the benzyl groups give rise to an AB spin system at 4.42 and 3.74 ppm with $^2J_{H\text{-}H}$ = 15 Hz. The resonances for the [C2] and [C3] chains of the macrocycle range between 3.15 and 1.87 ppm. The methylene

protons of the CH_2SiMe_3 group give rise to an AB spin system at −1.29 and −1.37 ppm with $^2J_{H\text{-}H}$ = 10 Hz. Comparable coupling constant values ($^2J_{H\text{-}H}$ = 11 Hz) are reported for alkyl yttrium complexes with linked 1,4,7-triazacyclononane-amido monoanionic ancillary ligands [81,82]. The integration of the resonances of **7** is consistent with one macrocycle per CH_2SiMe_3 ligand. The ten overlapped resonances integrate for the twenty methylene protons of the [C2] and [C3] chains of the cyclam ring. These protons correlate with five different carbon signals in the $^{13}C\{^1H\}$ NMR spectrum, as observed in the HSQC experiment (Figure S9). The carbon signal that corresponds to the methylene carbon of the CH_2SiMe_3 does not appear due to the coupling with yttrium, although it is evidenced by the correlation with the protons' resonances. The methyl carbon signals cannot be identified since they overlap with the signals of the ^{t}Bu groups and the starting material $Y(CH_2SiMe_3)_3(THF)_2$ that is not yet completely consumed at this stage. Slowly warming the solution up to room temperature revealed the formation of other species above −20 °C, attesting that the decomposition of **7** starts before the complete consumption of the reagents.

Preliminary catalytic assays have shown that [Y{(η^3-$^{3,5\text{-}tBu2}$Bn)$_2$Cyclam}Li(THF)], **6**, is a very efficient catalyst for the intramolecular hydroamination of 2,2-diphenyl-pent-4-enylamine. The substrate was fully converted into 2-methyl-4,4-diphenylpyrrolidine after 4 h at room temperature. Figure S10 shows the cyclization kinetic plot for the intramolecular hydroamination of 2,2-diphenyl-pent-4-enylamine catalyzed by **6**.

3. Materials and Methods

3.1. General Considerations

Compounds **1** [83], **5** [84], and 2,2-diphenyl-pent-4-enylamine [85] were prepared according to previously published procedures. All other reagents were commercial grade and used without purification. All manipulations were performed under an atmosphere of dry oxygen-free nitrogen by means of standard Schlenk and glovebox techniques. Solvents were pre-dried using 4 Å molecular sieves and refluxed over sodium-benzophenone under an atmosphere of N_2 and collected by distillation. Deuterated solvents were dried with 4 Å molecular sieves and freeze–pump–thaw degassed prior to use. NMR spectra were recorded in Bruker AVANCE II^{TM} 300 or 400 MHz spectrometers (Bruker BioSpin, Ettlingen, Germany) at 296 K, referenced internally to residual proton-solvent (^1H) or solvent (^{13}C) resonances, and reported relative to tetramethylsilane (0 ppm). ^{11}B NMR was referenced to external $BF_3.Et_2O$ (0 ppm). Two-dimensional NMR experiments such as ^1H-^{13}C HSQC and ^1H-^1H COSY were performed in order to make all the assignments. Elemental analyses (C, H, N) were performed in a Fisons CHNS/O analyzer Carlo Erba Instruments EA-1108 equipment (Carlo Erba Strumentazione, Milano, Italy) at the Laboratório de Análises do Instituto Superior Técnico.

3.2. Synthetic Procedures

[(Bn_2Cyclam)Y($N(SiMe_3)_2$)], **2**: 1,8-dibenzyl-1,4,8,11-tetraazacyclotetradecane, **1** (0.38 g, 1.00 mmol) was dissolved in THF (10 mL) and was added to a solution of $Y[N(SiMe_3)_2]_3$ (0.57 g, 1.00 mmol) in the same solvent. The reaction mixture was stirred at 50 °C overnight. Then, the solution was filtered off and the volatiles were removed under vacuum. The solid residue was washed with hexane and dried under vacuum to give compound **2** as a microcrystalline solid in 87% yield (0.55 g, 0.87 mmol). ^1H NMR (C_6D_6, 300.1 MHz, 296 K): δ (ppm) 7.12–7.00 (overlapping, 10H, *Ph*CH_2N), 4.51 (d, 2H, $^2J_{H\text{-}H}$ = 15 Hz, PhCH_2N), 4.15 (d, 2H, $^2J_{H\text{-}H}$ = 15 Hz, PhCH_2N), 3.35–3.28 (overlapping, 4H total, 2H, [C3]CH_2N and 2H, [C2]CH_2N), 3.22 (m, 2H, [C2]CH_2N), 3.10–2.96 (overlapping, 4H total, [C2]CH_2N), 2.85 (m, 2H, [C3]CH_2N), 2.38 (m, 2H, [C3]CH_2N), 2.32–2.19 (overlapping, 4H total, 2H, $CH_2CH_2CH_2$ and 2H, [C2]CH_2N), 1.68 (m, 2H, $CH_2CH_2CH_2$), 0.54 (s, 18H, NSi(CH_3)$_3$). $^{13}C\{^1H\}$ NMR (C_6D_6, 75.0 MHz, 295 K): δ (ppm) 132.0 (*Ph*CH_2N), 131.2 (*i-Ph*CH_2N), 128.5 (*Ph*CH_2N), 128.4 (*Ph*CH_2N), 58.6 (d, $^3J_{Y\text{-}C}$ = 2 Hz, [C2]CH_2N), 57.1 (PhCH_2N), 56.2 ([C3]CH_2N), 53.7 (d, $^3J_{Y\text{-}C}$ = 2 Hz, [C2]CH_2N), 46.8 ([C3]CH_2N), 27.3 ($CH_2CH_2CH_2$), 6.5 (NSi(CH_3)$_3$). Anal. Calc. for $C_{30}H_{52}N_5Si_2Y$: C, 57.39; H, 8.35; N, 11.15. Found: C, 56.98; H, 8,15; N, 10.93.

[(HBn$_2$Cyclam)Y(N(SiMe$_3$)$_2$)][BPh$_4$], **3**: [HNMe$_3$][BPh$_4$] (0.19 g, 0.50 mmol) was dissolved in THF (5 mL) and was added dropwise to a solution of **2** (0.28 g, 0.50 mmol) in the same solvent. The mixture was stirred overnight at room temperature. The solution was filtered off and was concentrated under vacuum. The concentrated solution was double-layered with toluene and it was left at −20 °C for two days, from which compound **3** was collected as crystalline material in 92% yield (0.44 g, 0.46 mmol). ^{1}H NMR (CD$_2$Cl$_2$, 400.1 MHz, 296 K): δ (ppm) 7.48 (m, 6H, *Ph*CH$_2$N), 7.39 (br, 8H, *o-Ph*-B), 7.22 (m, 4H, *Ph*CH$_2$N), 7.05 (t, 8H, $^3J_{H\text{-}H}$ = 8 Hz, *m-Ph*-B), 6.90 (t, 4H, $^3J_{H\text{-}H}$ = 8 Hz, *p-Ph*-B), 4.43 (d, 1H, $^2J_{H\text{-}H}$ = 14 Hz, PhC*H*$_2$N), 4.17 (d, 1H, $^2J_{H\text{-}H}$ = 14 Hz, PhC*H*$_2$N), 4.11 (d, 1H, $^2J_{H\text{-}H}$ = 14 Hz, PhC*H*$_2$N), 3.82 (d, 1H, $^2J_{H\text{-}H}$ = 14 Hz, PhC*H*$_2$N), 3.50 (m, 1H, [C2]C*H*$_2$N), 3.17 (m, 1H, [C2]C*H*$_2$N), 2.96–2.89 (m, 1H, [C3]C*H*$_2$N), 2.85–2.78 (overlapping, 2H total, 1H, [C3]C*H*$_2$N and 1H, [C3]C*H*$_2$N), 2.75–2.44 (overlapping, 8H total, [C3]C*H*$_2$N and [C2]C*H*$_2$N), 2.28 (m, 1H, [C3]C*H*$_2$N or [C2]C*H*$_2$N), 2.22–2.10 (overlapping, 3H total, 1H, [C3]C*H*$_2$N, 1H, CH$_2$C*H*$_2$CH$_2$ and 1H, [C3]C*H*$_2$N or [C2]C*H*$_2$N), 2.01 (m, 1H, CH$_2$C*H*$_2$CH$_2$), 1.61–1.55 (overlapping, 2H, CH$_2$C*H*$_2$CH$_2$), 0.22 (s, 9H, NSi(C*H*$_3$)$_3$), 0.21 (s, 9H, NSi(C*H*$_3$)$_3$). ^{13}C{^{1}H} NMR (CD$_2$Cl$_2$, 100.0 MHz, 296 K): δ (ppm) 164.6 (q, $^1J_{B\text{-}C}$ = 49 Hz, *i-Ph*B), 133.6 (*o-Ph*B), 132.3 (*Ph*CH$_2$N), 132.3 (*Ph*CH$_2$N), 130.1 (*Ph*CH$_2$N), 129.9 (*Ph*CH$_2$N), 129.5 (*Ph*CH$_2$N), 129.3 (*Ph*CH$_2$N), 128.9 (*i-Ph*CH$_2$N), 128.4 (*i-Ph*CH$_2$N), 126.3 (q, $^1J_{B\text{-}C}$ = 3 Hz, *m-Ph*B), 122.4 (*p-Ph*B), 57.1 (PhCH$_2$N), 56.9 (PhCH$_2$N), 56.2 (d, $^3J_{Y\text{-}C}$ = 2 Hz, [C3]CH$_2$N), 54.2 ([C3]CH$_2$N), 53.3 (d, $^3J_{Y\text{-}C}$ = 2 Hz, [C3]CH$_2$N or [C2]CH$_2$N), 52.0 ([C3]CH$_2$N or [C2]CH$_2$N), 51.9 ([C3]CH$_2$N or [C2]CH$_2$N), 51.4 ([C2]CH$_2$N), 48.4 ([C3]CH$_2$N or [C2]CH$_2$N), 47.4 ([C3]CH$_2$N), 27.3 (CH$_2$CH$_2$CH$_2$), 25.0 (CH$_2$CH$_2$CH$_2$), 5.5 (NSi(CH$_3$)$_3$), 5.3 (NSi(CH$_3$)$_3$). ^{11}B NMR (CD$_2$Cl$_2$, 96.2 MHz, 296 K): δ (ppm) −6.5 (s, *B*Ph$_4$). Anal. Calc. for C$_{54}$H$_{73}$BN$_5$Si$_2$Y.C$_4$H$_8$O: C, 68.28; H, 8.00; N, 6.86. Found: C, 67.88; H, 7.86; N, 6.64.

[Y{(η^3-$^{3,5\text{-}tBu2}$Bn)$_2$Cyclam}Li(THF)], **6**: A THF solution of LiCH$_2$SiMe$_3$ (424 mg, 4.50 mmol) was slowly added to a THF suspension of YCl$_3$ (293 mg, 1.50 mmol). The mixture was stirred for 1 h at room temperature. Then, the mixture was cooled to −20 °C and a THF solution of 1,8-bis(3,5-di-*tert*-butylbenzyl)-1,4,8,11-tetraazacyclotetradecane, **5** (908 mg, 1.50 mmol) was added dropwise. The mixture was allowed to warm up to room temperature and was left stirring overnight. The volatiles were removed under vacuum and the yellow residue was extracted with toluene followed by evaporation of the solvent to give a yellow solid in 26% yield (299 mg, 0.39 mmol). ^{1}H NMR (C$_6$D$_6$, 300.1 MHz, 296 K): δ (ppm) 6.56 (s, 2H, Ar-*H*$_{allyl}$), 6.15 (s, 2H, Ar-*H*$_{para}$), 4.77 (s, 2H, Ar-*H*), 4.05 (m, 2H, [C2]C*H*$_2$N), 3.89 (m, 2H, [C3]C*H*$_2$N), 3.67 (s, 2H, NC*H*Ar), 3.52 (m, 2H, [C3]C*H*$_2$N), 3.29 (br, 4H, *THF*), 3.03-2.91 (overlapping, 4H total, 2H, [C3]C*H*$_2$N and 2H, [C2]C*H*$_2$N), 2.70–2.60 (m, 4H, [C2]C*H*$_2$N), 2.10 (m, 2H, CH$_2$C*H*$_2$CH$_2$), 1.74 (m, 2H, CH$_2$C*H*$_2$CH$_2$), 1.59 (m, 2H, CH$_2$C*H*$_2$CH$_2$), 1.57 (s, 18H, C(C*H*$_3$)$_3$), 1.39 (s, 18H, C(C*H*$_3$)$_3$), 1.24 (br, 4H, *THF*). ^{13}C{^{1}H} NMR (C$_6$D$_6$, 75.5 MHz, 296 K): δ (ppm) 154.5 (*ipso*, Ar-^{t}Bu), 153.6 (*ipso*, Ar-^{t}Bu), 141.7 (*ipso*, Ar-CHN), 113.9 (Ar-H$_{allyl}$), 105.3 (Ar-H$_{para}$), 90.5 (Ar-H), 76.3 (d, $^3J_{Y\text{-}C}$ = 3.0 Hz, NCHAr), 68.6 (*THF*), 57.6 ([C2]CH$_2$N), 57.2 ([C3]CH$_2$N), 55.2 ([C2]CH$_2$N), 49.5 ([C3]CH$_2$N), 35.4 (*C*(CH$_3$)$_3$), 34.8 (*C*(CH$_3$)$_3$), 32.0 (C(*C*H$_3$)$_3$), 31.8 (C(*C*H$_3$)$_3$), 30.6 (CH$_2$CH$_2$CH$_2$), 25.4 (*THF*). Anal. Calc. for C$_{44}$H$_{72}$LiN$_4$OY: C, 68.73; H, 9.44; N, 7.29. Found: C, 68.67; H, 9.50; N, 7.18.

[($^{3,5\text{-}tBu2}$Bn$_2$Cyclam)Y(CH$_2$SiMe$_3$)], **7**: Y(CH$_2$SiMe$_3$)$_3$(THF)$_2$ (15.0 mg, 0.03 mmol) was dissolved in THF-d$_8$, transferred into an NMR tube under an oxygen-free nitrogen atmosphere and frozen with a liquid nitrogen bath. A solution of 1,8-bis(3,5-di-*tert*-butylbenzyl)-1,4,8,11-tetraazacyclotetradecane, **5** (18.0 mg, 0.03 mmol) in the same solvent was layered on the top of the latter frozen solution. The mixture of solutions was frozen with liquid nitrogen and it was degassed under vacuum. The NMR tube was sealed with the system under vacuum and was left to warm up to −80 °C. A variable temperature ^{1}H NMR experiment was performed and the formation of compound **7** was detected at −30 °C. At this temperature, ^{13}C{^{1}H} and 2D NMR spectra were performed to confirm the formation of compound **7**. The product was extremely unstable and its decomposition was observed in 8 h at −20 °C. ^{1}H NMR (THF-d$_8$, 300.1 MHz, 243 K): δ (ppm) 7.39 (s, 2H,

p-*Ph*CH_2N), 7.07 (s, 4H, *o*-*Ph*CH_2N), 4.42 (d, 2H, $^2J_{H\text{-}H}$ = 15 Hz, PhCH_2N), 3.74 (d, 2H, $^2J_{H\text{-}H}$ = 15 Hz, PhCH_2N), 3.15 (overlapping, 4H total, 2H, [C3]CH_2N and 2H, [C2]CH_2N), 2.96 (m, 2H, [C2]CH_2N), 2.85 (overlapping, 4H total, [C2]CH_2N), 2.68 (overlapping, 4H, 2H, [C3]CH_2N and 2H, [C3]CH_2N), 2.35–2.26 (overlapping, 4H total, 2H, $CH_2CH_2CH_2$ and 2H, [C2]CH_2N), 1.87 (m, 2H, $CH_2CH_2CH_2$), 1.29 (br, 36H, C(CH_3)$_3$), −0.92 (s, 9H, Si(CH_3)$_3$), −1.29 (d, 2H, $^2J_{H\text{-}H}$ = 10 Hz, YCH_2SiMe_3), −1.37 (d, 2H, $^2J_{H\text{-}H}$ = 10 Hz, YCH_2SiMe_3). $^{13}C\{^1H\}$ NMR (THF-d_8, 75.0 MHz, 243 K): δ (ppm) 150.9 (*m*-*Ph*CH_2N), 150.5 (*m*-*Ph*CH_2N), 131.5 (*i*-*Ph*CH_2N), 126.9 (*o*-*Ph*CH_2N), 122.5 (*p*-*Ph*CH_2N), 58.9 ([C2]CH_2N), 58.2 (PhCH_2N), 56.9 ([C3]CH_2N), 55.0 ([C2]CH_2N), 47.3 ([C3]CH_2N), 35.4 (*C*(CH_3)$_3$), 31.9 (C(CH_3)$_3$ and (Si(CH_3)$_3$), 27.5 ($CH_2CH_2CH_2$), 21.2 (br, YCH_2SiMe_3).

3.3. Catalytic Assays

Hydroamination reactions were carried out in an N_2-filled glovebox on an NMR-tube scale. 2,2-diphenyl-pent-4-enylamine, 1,3,5-trimethoxybenzene, and the catalyst were dissolved in toluene-d_8. The resulting solutions were placed in NMR tubes equipped with a Teflon screw cap. The reaction progress was monitored by ^1H NMR spectroscopy.

3.4. Single-Crystal X-ray Diffraction Studies

Suitable crystals of compounds **2**–**4** and **6** were coated and selected in Fomblin® Y oil (Sigma-Aldrich, Steinheim, Germany) under an inert atmosphere of nitrogen. Crystals were then mounted on a loop external to the glovebox environment and data were collected using graphite monochromated Mo-Kα radiation (λ = 0.71073 Å) on a Bruker AXS-KAPPA APEX II diffractometer (Bruker AXS, Karlsruhe, Germany) equipped with an Oxford Cryosystem open-flow nitrogen cryostat operating at 150(2) K. Data were corrected for Lorentzian polarization and absorption effects using SAINT [86] and SADABS [87] programs. The structures were solved by direct methods using SIR92 [88] and SIR97 [89]. Structure refinement was conducted using SHELXL-2018/3 [90]. These programs are part of the WinGX-Version 2021.3 program package [91]. Hydrogen atoms bonded to carbons were inserted in idealized positions and allowed to refine in the parent carbon atom. Hydrogen atoms of N*H* moieties were located in the electron density map and refined freely. Compounds **3** and **6** crystallized with diffuse and disordered solvent molecules that could not be modeled. Therefore, they were removed using the PLATON/Squeeze sequence [92]. A total void of 892 $Å^3$ containing 356 electrons per unit cell was found for **3** and fits well for four molecules of THF (40 electrons). A total void of 1362 $Å^3$ containing 376 electrons per unit cell was found for **6** and fits well for two molecules of toluene (50 electrons). The poor diffracting power and crystal quality of compounds **3** and **4** also precluded the final refinement to lower the *R* values. Crystallographic and experimental details of data collection and crystal structure determinations are available in Table S1. Illustrations of the molecular structures were made with MERCURY 2022.3.0 [93]. Data for structures **2**–**4** and **6** were deposited in the Cambridge Crystallographic Data Centre (CCDC) under the deposit numbers 2294327–2294330, respectively.

3.5. Computational Studies

Density Functional Theory calculations [94] were performed using the Gaussian 09 software package [95] and M06 functional without symmetry constraints that is a hybrid meta-GGA functional developed by Truhlar and Zhao [96], and it was shown to perform very well for transition metal systems, providing a good description of weak and long-range interactions [97,98]. The basis set used for the geometry optimizations consisted of a LanL2DZ set [99–102] augmented with an f-polarization function [103] for yttrium and a standard 6-31G** [104–108] for the remaining elements. A Natural Population Analysis (NPA) [51–56] and the resulting Wiberg indices [109] were used to study the electronic structure and bonding of the optimized species.

4. Conclusions

New Y(III) complexes supported by *trans-N,N′*-disubstituted cyclam ligands were synthesized and characterized. [(Bn_2Cyclam)Y($N(SiMe_3)_2$)] was readily protonated with [$HNMe_3$][BPh_4] to give [(HBn_2Cyclam)Y($N(SiMe_3)_2$)][BPh_4]. DFT analysis of [(Bn_2Cyclam)Y($N(SiMe_3)_2$)] showed that the HOMO is located on the anionic nitrogen atoms of the cyclam ring and thus the protonation reaction follows orbital control. The addition of H_2Bn_2Cyclam and $H_2(^{3,5\text{-}tBu2}Bn)_2$Cyclam to a 1:3 mixture of YCl_3 and $LiCH_2SiMe_3$ in THF resulted in the formation of [$((C_6H_4CH_2)$BnCyclam)Y(THF)(μ-Cl)Li$(THF)_2$] and [Y{$(\eta^3\text{-}^{3,5\text{-}tBu2}Bn)_2$Cyclam}Li(THF)]. The presence of lithium in both compounds seems to be critical not only for the stabilization of the complexes but also for the stabilization of reaction intermediates. Complexes [$((C_6H_4CH_2)$BnCyclam)Y(THF)(μ-Cl)Li$(THF)_2$] and [Y{$(\eta^3\text{-}^{3,5\text{-}tBu2}Bn)_2$Cyclam}Li(THF)] were formed through C-H activation reactions involving the intramolecular elimination of tetramethylsilane. The substituents of the benzyl pending arms of cyclam have a crucial effect on the C-H bonds that are cleaved. The reaction of $Y(CH_2SiMe_3)_3(THF)_2$ with $H_2(^{3,5\text{-}tBu2}Bn)_2$Cyclam was studied and monitored by a temperature variation NMR experiment revealing that [$(^{3,5\text{-}tBu2}Bn_2$Cyclam)Y(CH_2SiMe_3)] is formed. This species is unstable and undergoes decomposition above −20 °C into unidentified species that are responsible for the extreme difficulty in the preparation and isolation of yttrium alkyl complexes anchored on cyclam ligands. Preliminary catalytic assays have shown that [Y{$(\eta^3\text{-}^{3,5\text{-}tBu2}Bn)_2$Cyclam}Li(THF)] is a very efficient catalyst for the intramolecular hydroamination of 2,2-diphenyl-pent-4-enylamine.

Supplementary Materials: The following supporting information can be downloaded at: https://www.mdpi.com/article/10.3390/molecules28247998/s1, Figures S1, S3–S9: NMR spectra; Figure S2: SCRXD molecular structure of **3**; Figure S10: Cyclization kinetic plot; Table S1: Crystal data and structure refinement.

Author Contributions: Conceptualization, A.M.M.; synthesis and characterization: F.M. and L.G.A.; catalytic assays and SCRXD studies: L.G.A.; DFT studies: F.M. and L.F.V.; writing—original draft preparation, F.M. and L.G.A.; writing—review and editing, L.F.V. and A.M.M.; supervision, L.F.V. and A.M.M. All authors have read and agreed to the published version of the manuscript.

Funding: This research was funded by Fundação para a Ciência e a Tecnologia, Portugal (UID/QUI/00100/2019, UIDB/00100/2020, UIDP/00100/2020, LA/P/0056/2020 and SFRH/BD/87679/2012).

Data Availability Statement: The data presented in this study are available in Supplementary Material.

Conflicts of Interest: The authors declare no conflict of interest.

References

1. Trifonov, A.A.; Lyubov, D.M.A. A quarter-century long story of bis(alkyl) rare-earth (III) complexes. *Coord. Chem. Rev.* **2017**, *340*, 10–61. [CrossRef]
2. Manβen, M.; Schafer, L.L. Early Transition Metal-Catalyzed Hydroamination. *Trends Chem.* **2021**, *3*, 428–429.
3. Lovick, H.M.; An, D.K.; Livinghouse, T.S. Structure-activity relationships in group 3 metal catalysts for asymmetric intramolecular alkenehydroamination. An investigation of ligands based on the axially chiral 1,1′-binaphthyl-2,2′-diamine motif. *Dalton Trans.* **2011**, *40*, 7697–7700. [CrossRef] [PubMed]
4. Chapurina, Y.; Guillot, R.; Lyubov, D.; Trifonov, A.; Hannedouche, J.; Schultz, E. LiCl-effect on asymmetric intramolecular hydroamination catalyzed by binaphthylamido yttrium complexes. *Dalton Trans.* **2013**, *42*, 507–520. [CrossRef] [PubMed]
5. Lauterwasser, F.; Hayes, P.G.; Piers, W.E.; Schafer, L.L.; Bräse, S. Highly Active and Diastereoselective *N,O*- and *N,N*-Yttrium Complexes for Intramolecular Hydroamination. *Adv. Synth. Catal.* **2011**, *353*, 1384–1390. [CrossRef]
6. Aillaud, I.; Collin, J.; Hannedouche, J.; Schulz, E.; Trifonov, A. Comparison of yttrium binaphthylamido alkyl and amide complexes for enantioselective intramolecular hydroamination. *Tetrahedron Lett.* **2010**, *51*, 4742–4745. [CrossRef]
7. Reznichenko, A.L.; Hultzsch, K.C. C_1-Symmetric Rare-Earth-Metal Aminodiolate Complexes for Intra- and Intermolecular Asymmetric Hydroamination of Alkenes. *Organometallics* **2013**, *32*, 1394–1408. [CrossRef]
8. Nguyen, H.N.; Lee, H.; Audörsch, S.; Reznichenko, A.L.; Nawara-Hultzsch, A.J.; Schmidt, B.; Hultzsch, K.C. Asymmetric Intra- and Intermolecular Hydroamination Catalyzed by 3,3′-Bis(trisarylsilyl)- and 3,3′-Bis(arylalkylsilyl)-Substituted Binaphtholate Rare-Earth-Metal Complexes. *Organometallics* **2018**, *37*, 4358–4379. [CrossRef]

9. Nguyen, H.N.; Hultzsch, K.C. Rare-Earth-Metal-Catalyzed Kinetic Resolution of Chiral Aminoalkenes via Hydroamination: The Effect of the Silyl Substituent of the Binaphtholate Ligand on Resolution Efficiency. *Eur. J. Org. Chem.* **2019**, *2019*, 2592–2601. [CrossRef] [PubMed]
10. Nawara-Hultzsch, A.J.; Goswami, A.; Hultzsch, K.C. Effect of Additives in the Hydroamination/Cyclization of Aminoalkenes Catalyzed by a Binaphtholate Yttrium Catalyst. *Adv. Syn. Cat.* **2023**, *365*, 568–578. [CrossRef]
11. Kissel, A.A.; Lyubov, D.M.; Mahrova, T.V.; Fukin, G.K.; Cherkasov, A.V.; Glukhova, T.A.; Cuib, D.; Trifonov, A.A. Rare-earth dichloro and bis(alkyl) complexes supported by bulky amido-iminoligand. Synthesis, structure, reactivity and catalytic activity in isoprene polymerization. *Dalton Trans.* **2013**, *42*, 9211–9225. [CrossRef] [PubMed]
12. Rad'kova, N.Y.; Skvortsov, G.G.; Cherkasov, A.V.; Fukin, G.K.; Kovylina, T.A.; Ob'edkov, A.M.; Trifonov, A.A. Bis(alkyl) Sc and Y Complexes Supported by Tri- and Tetradentate Amidinate Ligands: Synthesis, Structure, and Catalytic Activity in α-Olefin and Isoprene Polymerization. *Eur. J. Inorg. Chem.* **2021**, *2021*, 2365–2373. [CrossRef]
13. Tolpygin, A.O.; Sachkova, A.A.; Mikhailychev, A.D.; Ob'edkov, A.M.; Kovylina, T.A.; Cherkasov, A.V.; Fukin, G.K.; Trifonov, A.A. Sc and Y bis(alkyl) complexes supported by bidentate and tridentate amidinate ligands. Synthesis, structure and catalytic activity in polymerization of isoprene and 1-heptene. *Dalton Trans.* **2022**, *51*, 7723–7731. [CrossRef]
14. Luconi, L.; Kissel, A.A.; Rossin, A.; Khamaletdinova, N.M.; Cherkasov, A.V.; Tuci, G.; Fukin, G.K.; Trifonov, A.A.; Giambastiani, G. C_1 and C_S 2-pyridylethylanilido zirconium(IV), yttrium(III) and lutetium(III) complexes: Synthesis, characterization and catalytic activity in the isoprene polymerization. *New J. Chem.* **2017**, *41*, 540–551. [CrossRef]
15. Lyubov, D.M.; Tolpygin, A.O.; Trifonov, A.A. Rare-earth metal complexes as catalysts for ring-opening polymerization of cyclic esters. *Coord. Chem. Rev.* **2019**, *392*, 83–145. [CrossRef]
16. Skvortsov, G.G.; Cherkasov, A.V.; Vorozhtsov, D.L.; Shchegravina, E.S.; Trifonov, A.A. Yttrium and Lithium Keto-β-Diketiminate Complexes $[\{2,6\text{-}Me_2C_6H_3N{=}C(Me)\}_2CC(tert\text{-}Bu){=}O]_2Y(\mu^2\text{-}Cl)_2Li(THF)_2$ and $\{[\{2,6\text{-}Me_2C_6H_3N{=}C(Me)\}_2CC(tert\text{-}Bu){=}O]Li(THF)\}_n$. Synthesis, and Catalytic Activity in ε-Caprolactone Polymerization. *Russ. J. Coord. Chem.* **2021**, *47*, 144–154. [CrossRef]
17. Fanq, J.; Tschan, M.J.-L.; Roisnel, T.; Trivelli, X.; Gauvin, R.M.; Thomas, C.M.; Maron, L. Yttrium catalysts for syndioselective β-butyrolactone polymerization: On the origin of ligand-induced stereoselectivity. *Polym. Chem.* **2013**, *4*, 360–367. [CrossRef]
18. Mazzeo, M.; Tramontano, R.; Lamberti, M.; Pilone, A.; Milione, S.; Pellecchia, C. Rare earth complexes of phenoxy-thioetherligands: Synthesis and reactivity in the ring opening polymerization of cyclic esters. *Dalton Trans.* **2013**, *42*, 9338–9351. [CrossRef]
19. Li, G.; Lamberti, M.; Mazzeo, M.; Pappalardo, D.; Roviello, G.; Pellecchia, C. Anilidopyridyl-Pyrrolide and Anilidopyridyl-Indolide Group 3 Metal Complexes: Highly Active Initiators for the Ring-Opening Polymerization of *rac*-Lactide. *Organometallics* **2012**, *31*, 1180–1188. [CrossRef]
20. Bakewell, C.; Cao, T.-P.-A.; Long, N.; Goff, X.F.L.; Auffrant, A.; Williams, C.K. Yttrium Phosphasalen Initiators for *rac*-Lactide Polymerization: Excellent Rates and High Iso-Selectives. *J. Am. Chem. Soc.* **2012**, *134*, 20577–20580. [CrossRef]
21. Venugopal, A.; Fegler, W.; Spaniol, T.P.; Maron, L.; Okuda, J. Dihydrogen Addition in a Dinuclear Rare-Earth Metal Hydride Complex Supported by a Metalated TREN Ligand. *J. Am. Chem. Soc.* **2011**, *133*, 17574–17577. [CrossRef]
22. Jie, S.; Diaconescu, P.L. Reactions of Aromatic N-Heterocycles with Yttrium and Lutetium Benzyl Complexes Supported by a Pyridine-Diamine Ligand. *Organometallics* **2010**, *29*, 1222–1230. [CrossRef]
23. Lu, E.; Gan, W.; Chen, Y. Monoalkyl and monoanilide yttrium complexes containing tridentate pyridyl-1-azaallyl dianionic ligands. *Dalton Trans.* **2011**, *40*, 2366–2374. [CrossRef] [PubMed]
24. Basalov, I.V.; Kissel, A.A.; Nikolaevskaya, E.N.; Druzhkov, N.O.; Cherkasov, A.V.; Long, J.; Larionova, J.; Fukina, G.K.; Trifonov, A.A. 2-Imino-2,3-dihydrobenzoxazole-a useful platform for designing rare- and alkaline earth complexes with variable di- and trianionic O,N,N, ligands. *Dalton Trans.* **2022**, *51*, 1995–2004. [CrossRef] [PubMed]
25. Fayoumi, A.; Lyubov, D.M.; Tolpygin, A.O.; Shavyrin, A.S.; Cherkasov, A.V.; Ob'edkov, A.M.; Trifonov, A.A. Sc and Y Heteroalkyl Complexes with a $NC_{sp3}N$ Pincer-Type Diphenylmethanido Ligand: Synthesis, Structure, and Reactivity. *Eur. J. Inorg. Chem.* **2020**, *2020*, 3259–3267. [CrossRef]
26. Skvortsov, G.G.; Cherkasov, A.V.; Fukin, G.K.; Trifonov, A.A. Yttrium complexes containing heteroscorpionate ligands $[(3,5\text{-}Bu^t_2C_3HN_2)_2CHC(Ph)_2O]^-$ and $[o\text{-}Me_2NC_6H_4CH_2C(NCy)_2]^-$. *Russ. Chem. Bull.* **2016**, *65*, 1189–1197. [CrossRef]
27. Luconi, L.; Lyubov, D.M.; Bianchini, C.; Rossin, A.; Faggi, C.; Fukin, G.K.; Cherkasov, A.V.; Shavyrin, A.S.; Trifonov, A.A.; Giambastiani, G. Yttrium-Amidopyridinate Complexes: Synthesis and Characterization of Yttrium-Alkyl and Yttrium-Hydrido Derivatives. Eur. *J. Inorg. Chem.* **2010**, *2010*, 608–620. [CrossRef]
28. Karpov, A.A.; Cherkasov, A.V.; Fukin, G.K.; Shavyrin, A.S.; Luconi, L.; Giambastini, G.; Trifonov, A.A. Yttrium Complexes Featuring Different Y-C Bonds. Comparative Reactivity Studies: Toward Terminal Imido Complexes. *Organometallics* **2013**, *32*, 2379–2388. [CrossRef]
29. Cui, P.; Spaniol, T.P.; Okuda, J. Heterometallic Potassium Rare-Earth-Metal Allyl and Hydrido Complexes Stabilized by a Dianionic (NNNN)-Type Macrocyclic Ancillary Ligand. *Organometallics* **2013**, *32*, 1176–1182. [CrossRef]
30. Cui, P.; Spaniol, T.P.; Maron, L.; Okuda, J. An ion pair scandium hydride supported by a dianionic (NNNN)-type macrocycle ligand. *Chem. Commun.* **2014**, *50*, 424–426. [CrossRef] [PubMed]
31. Kulina, H.; Spaniol, T.P.; Okuda, J. Neutral and Cationic Zirconium Hydrides Supported by a Dianionic (NNNN)-Type Macrocycle Ligand. *Organometallics* **2015**, *34*, 2160–2164. [CrossRef]

32. Munhá, R.F.; Ballmann, J.; Veiros, L.F.; Patrick, B.O.; Fryzuk, M.D.; Martins, A.M. Dinuclear Cationic Zirconium Hydrides Stabilized by the *N,N*-Dibenzylcyclam Ancillary Ligand. *Organometallics* **2012**, *31*, 4937–4940. [CrossRef]
33. Munhá, R.F.; Veiros, L.F.; Duarte, M.T.; Fryzuk, M.D.; Martins, A.M. Synthesis and structural studies of amido, hydrazido and imido zirconium(IV) complexes incorporating a diamido/diamine cyclam-based ligand. *Dalton Trans.* **2009**, *36*, 7494–7508. [CrossRef]
34. Alves, L.G.; Martins, A.M. Synthesis and Characterization of New Cyclam-Based Zr(IV) Alkoxido Derivatives. *Reactions* **2021**, *2*, 323–332. [CrossRef]
35. Alves, L.G.; Munhá, R.F.; Martins, A.M. Synthesis and reactivity of cyclam-based Zr(IV) complexes. *Inorg. Chim. Acta* **2019**, *490*, 204–214. [CrossRef]
36. Munhá, R.F.; Antunes, M.A.; Alves, L.G.; Veiros, L.F.; Fryzuk, M.D.; Martins, A.M. Structure and Reactivity of Neutral and Cationic *trans-N,N′*-Dibenzylcyclam Zirconium Alkyl Complexes. *Organometallics* **2010**, *29*, 3753–3764. [CrossRef]
37. Alves, L.G.; Antunes, M.A.; Matos, I.; Munhá, R.F.; Duarte, M.T.; Fernandes, A.C.; Marques, M.M.; Martins, A.M. Reactivity of a new family of diamido-diamine cyclam-based zirconium complexes in ethylene polymerization. *Inorg. Chim. Acta* **2010**, *363*, 1823–1830. [CrossRef]
38. Alves, L.G.; Hild, F.; Munhá, R.F.; Veiros, L.F.; Dagorne, S.; Martins, A.M. Synthesis and structural characterization of novel cyclam-based zirconium complexes and their use in the controlled ROP of *rac*-lactide: Access to cyclam-functionalized polylactide materials. *Dalton Trans.* **2012**, *41*, 14288–14298. [CrossRef]
39. Alves, L.G.; Madeira, F.; Munhá, R.F.; Barroso, S.; Veiros, L.F.; Martins, A.M. Reactions of heteroallenes with cyclam-based Zr(IV) complexes. *Dalton Trans.* **2015**, *44*, 1441–1455. [CrossRef]
40. Alves, L.G.; Madeira, F.; Munhá, R.F.; Maulide, N.; Veiros, L.F.; Martins, A.M. Cooperative Metal-Ligand Hydroamination Catalysis Supported by C-H Activation in Cyclam Zr(IV) Complexes. *Inorg. Chem.* **2018**, *57*, 13034–13045. [CrossRef]
41. Addison, A.W.; Rao, T.N.; Reedijk, J.; van Rijn, J.; Verschoor, G.C. Synthesis, structure, and spectroscopic properties of copper(II) compounds containing nitrogen-sulphur donor ligands; the crystal and molecular structure of aqua[1,7-bis(*N*-methylbenzimidazol-2′-yl)-2,6-dithiaheptane]copper(II) perchlorate. *J. Chem. Soc. Dalton Trans.* **1984**, 1349–1356. [CrossRef]
42. Lu, E.; Chen, Y.; Leng, X. Yttrium Anilido Hydride: Synthesis, Structure, and Reactivity. *Organometallics* **2011**, *30*, 5433–5441. [CrossRef]
43. Skinner, M.E.G.; Mountford, P. Scandium and yttrium complexes of the diamide-diamine donor ligand (2-C_5H_4N)$CH_2N(CH_2CH_2NSiMe_3)_2$: Chloride, primary and secondary amide, benzamidinate and alkyl functionalized derivatives. *J. Chem. Soc. Dalton Trans.* **2002**, 1694–1703. [CrossRef]
44. Zhang, X.; Zhou, S.; Fang, X.; Zhang, L.; Tao, G.; Wei, Y.; Zhu, X.; Cui, P.; Wang, S. Syntheses of Dianionic α-Iminopyridine Rare-Earth Metal Complexes and Their Catalytic Activities toward Dehydrogenative Coupling of Amines with Hydrosilanes. *Inorg. Chem.* **2020**, *59*, 9683–9692. [CrossRef] [PubMed]
45. Vitanova, D.V.; Hampel, F.; Hultzsch, K.C. Rare earth metal complexes based on β-diketiminato and novel linked bis(β-diketiminato) ligands: Synthesis, structural characterization and catalytic application in epoxide/CO_2-copolymerization. *J. Organomet. Chem.* **2005**, *690*, 5182–5197. [CrossRef]
46. Vitanova, D.V.; Hampel, F.; Hultzsch, K.C. Linked bis(β-diketiminato) yttrium and lanthanum complexes as catalysts in asymmetric hydroamination/cyclization of aminoalkenes (AHA). *J. Organomet. Chem.* **2011**, *696*, 321–330. [CrossRef]
47. Matsuo, Y.; Mashima, K.; Tani, K. Selective Formation of Homoleptic and Heteroleptic 2,5-Bis(*N*-aryliminomathyl)pyrrolyl Yttrium Complexes and Their Performance as Initiators of ε-Caprolactone Polymerization. *Organometallics* **2001**, *20*, 3510–3518. [CrossRef]
48. Benndorf, P.; Kratsh, J.; Hartenstein, L.; Preuss, C.M.; Roesky, P.W. Chiral Benzamidinate Ligands in Rare-Earth-Metal Coordination Chemistry. *Chem. Eur. J.* **2012**, *18*, 14454–14463. [CrossRef]
49. Arnold, P.L.; Cadenbach, T.; Marr, I.H.; Fyfe, A.A.; Bell, N.L.; Bellabarba, R.; Tooze, R.P.; Love, J.B. Homo- and heteroleptic alkoxycarbene f-element complexes and their reactivity towards acidic N-H and C-H bonds. *Dalton Trans.* **2014**, *43*, 14346–14358. [CrossRef]
50. Deelman, B.-J.; Booij, M.; Meetsma, A.; Teuben, J.H.; Kooijman, H.; Spek, A.L. Activation of Ethers and Sulfides by Organolanthanide Hydrides. Molecular Structures of (Cp*2Y)2(.mu.-OCH2CH2O)(THF)2 and (Cp*2Ce)2(.mu.-O)(THF)2. *Organometallics* **1995**, *14*, 2306–2317. [CrossRef]
51. Carpenter, J.E.; Weinhold, F. Analysis of the geometry of the hydroxymethyl radical by the "different hybrids for different spins" natural bond orbital procedure. *J. Mol. Struct. (Theochem)* **1988**, *169*, 41–62. [CrossRef]
52. Foster, J.P.; Weinhold, F. Natural hybrid orbitals. *J. Am. Chem. Soc.* **1980**, *102*, 7211–7218. [CrossRef]
53. Reed, A.E.; Weinhold, F. Natural bond orbital analysis of near-Hartree-Fock water dimer. *J. Chem. Phys.* **1983**, *78*, 4066–4073. [CrossRef]
54. Reed, A.E.; Weinstock, R.B.; Weinhold, F. Natural population analysis. *J. Chem. Phys.* **1985**, *83*, 735–746. [CrossRef]
55. Reed, A.E.; Curtis, L.A.; Weinhold, F. Intermolecular interactions from a natural bond orbital, donor-acceptor viewpoint. *Chem. Rev.* **1988**, *88*, 899–926. [CrossRef]
56. Weinhold, F.; Carpenter, J.E. The Natural Bond Orbital Lewis Structure Concept for Molecules, Radicals, and Radical Ions. In *The Structure of Small Molecules and Ions*; Naaman, R., Vager, Z., Eds.; Springer: Boston, MA, USA, 1988; pp. 227–236.

57. Lin, M.-H.; RajanBabu, T.V. Ligand-assisted rate acceleration in transacylation by a yttrium-salen complex. Demonstration of a conceptually new strategy for metal-catalyzed kinetic resolution of alcohols. *Org. Lett.* **2002**, *4*, 1607–1610. [CrossRef] [PubMed]
58. Martins, A.M.; Ascenso, J.R.; Costa, S.M.B.; Dias, A.R.; Ferreira, H.; Ferreira, J.A. Ion Pairing in Ti(IV) Trisamidotriazacyclononane Compounds. *Inorg. Chem.* **2005**, *44*, 9017–9022. [CrossRef]
59. Meyer, E.A.; Castellano, R.K.; Diederich, F. Interactions with Aromatic Rings in Chemical and Biological Recognition. *Angew. Chemie Int. Ed.* **2003**, *42*, 1210–1250. [CrossRef]
60. Liu, X.; Shang, X.; Tang, T.; Hu, N.; Pei, F.; Cui, D.; Chen, X.; Jing, X. Achiral Lanthanide Alkyl Complexes Bearing N,O Multidentate Ligands. Synthesis and Catalysis of Highly Heteroselective Ring-Opening Polymerization of *rac*-Lactide. *Organometallics* **2007**, *26*, 2747–2757. [CrossRef]
61. Maria, L.; Santos, I.C.; Alves, L.G.; Marçalo, J.; Martins, A.M. Rare earth metal complexes anchored on a new dianionic bis(phenolate)dimethylamine Cyclam ligand. *J. Organomet. Chem.* **2013**, *728*, 57–67. [CrossRef]
62. Song, G.; Luo, G.; Oyamada, J.; Luo, Y.; Hou, Z. *ortho*-Selective C-H addition of *N*,*N*-dimethyl anilides to alkenes by a yttrium catalyst. *Chem. Sci.* **2016**, *7*, 5265–5270. [CrossRef] [PubMed]
63. Wong, E.W.Y.; Das, A.K.; Katz, M.J.; Nishimura, Y.; Batchelor, R.J.; Onishi, M.; Leznoff, D.B. Diamidosilylether complexes of yttrium(III) and chromium(III): Synthetic challenges and surprises. *Inorg. Chim. Acta* **2006**, *359*, 2826–2834. [CrossRef]
64. Rastätter, M.; Muterle, R.B.; Roesky, P.W.; Thiele, S.K.-H. Bis(amido)cyclodiphosph(III)azane Complexes of Yttrium and the Lanthanides. *Chem. Eur. J.* **2009**, *15*, 474–481. [CrossRef]
65. Hultzsch, K.C.; Hampel, F.; Wagner, T. New yttrium complexes bearing diamidoamine ligands as efficient and diastereoselective catalysts for the intramolecular hydroamination of alkenes and alkynes. *Organometallics* **2004**, *23*, 2601–2612. [CrossRef]
66. Barroso, S.; Cui, J.; Carretas, J.M.; Cruz, A.; Santos, I.C.; Duarte, M.T.; Telo, J.P.; Marques, N.; Martins, A.M. Diamine Bis(phenolate) M(III) (Y, Ti) Complexes: Synthesis, Structures, and Reactivity. *Organometallics* **2009**, *28*, 3449–3458. [CrossRef]
67. Zhu, L.; Dong, Y.; Yin, B.; Ma, P.; Li, D. Improving the single-molecule magnet properties of two pentagonal bipyramidal Dy^{3+} compounds by the introduction of both electron-withdrawing and -donating groups. *Dalton Trans.* **2021**, *50*, 12607–12618. [CrossRef] [PubMed]
68. Wells, A.F. *Structural Inorganic Chemistry*, 5th ed.; Oxford University Press: Oxford, UK, 1984.
69. Shannon, R.D. Revised effective ionic radii and systematic studies of interatomic distances in halides and chalcogenides. *Acta Cryst.* **1976**, *A32*, 751–767. [CrossRef]
70. Mahrova, T.V.; Fukin, G.K.; Cherkasov, A.V.; Trifonov, A.A.; Ajellal, N.; Carpentier, J.-F. Yttrium Complexes Supported by Linked Bis(amide) Ligand: Synthesis, Structure, and Catalytic Activity in the Ring-Opening Polymerization of Cyclic Esters. *Inorg. Chem.* **2009**, *48*, 4258–4266. [CrossRef]
71. Ge, S.; Bambirra, S.; Meetsma, A.; Hessen, B. The 6-amino-6-methyl-1,4-diazepine group as na ancillary ligand framework forneutral and cationic scandium and yttrium alkyls. *Chem. Commun.* **2006**, 3320–3322. [CrossRef] [PubMed]
72. Wang, L.; Liu, D.; Cui, D. NNN-Tridentate Pyrrolyl Rare-Earth Metal Complexes: Structure and Catalysis on Specific Selective Living Polymerization of Isoprene. *Organometallics* **2012**, *31*, 6014–6021. [CrossRef]
73. Hillesheim, N.S.; Elfferding, M.; Linder, T.; Sundermeyer, J. New Cyclopentadienyl-*N*-Silylphosphazene Complexes of Rare-Earth Metals Yttrium and Lutetium. *Z. Anorg. Allg. Chem.* **2010**, *636*, 1776–1782. [CrossRef]
74. Zhu, X.; Li, Y.; Wei, Y.; Wang, S.; Zhou, S.; Zhang, L. Reactivity of 3-Imino-Functionalized Indoles with Rare-Earth-Metal Amides: Unexpected Substituent Effects on C-H Activation Pathways and Assembly of Rare-Earth-Metal Complexes. *Organometallics* **2016**, *35*, 1838–1846. [CrossRef]
75. Hultzsch, K.C.; Spaniol, T.P.; Okuda, J. Synthesis and Characterization of Yttrium Complexes Containing a Tridentate Linked Amido-Cyclopentadienyl Ligand. *Organometallics* **1998**, *17*, 485–488. [CrossRef]
76. Martins, A.M.; Munhá, R.F.; Alves, L.G.; Bharathi, S. A new family of zirconium complexes anchored by dianionic cyclam-based ligands: Syntheses, Structures, and Catalytic Applications. In *Advances in Organometallic Chemistry: The Silver/Gold Jubilee International Conference on Organometallic Chemistry Celebratory Book*; Pombeiro, J.L., Ed.; John Wiley & Sons, Inc.: Hoboken, NJ, USA, 2004; pp. 315–323.
77. Westerhausen, M.; Hartmann, M.; Pfitzner, A.; Schwarz, W. Bis(trimethylsilyl)amide und -methanide des Yttriums—Molekülstrukturen von Tris(diethylether-O)lithium-(μ-chloro)-tris[bis(trimethylsilyl)methyl]yttriat, solvensfreiem Yttrium-tris[bis(trimethylsilyl)amid] sowie dem Bis(benzonitrile)-Komplex. *Z. Anorg. Allg. Chem.* **1995**, *621*, 837–850. [CrossRef]
78. Evans, W.J.; Shreeve, J.L.; Broomhall-Dillard, R.N.R.; Ziller, J.W. Isolation and structure of a homoleptic yttrium trimethylsilylmethyl complex. *J. Organomet. Chem.* **1995**, *501*, 7–11. [CrossRef]
79. Wei, X.; Cheng, Y.; Hitchcock, P.B.; Lappert, M.F. Syntheses, structures and reactions of a series of β-diketiminatoyttrium compounds. *Dalton Trans.* **2008**, 5235–5246. [CrossRef] [PubMed]
80. Behrle, A.C.; Schmidt, J.A.R. Synthesis and Reactivity of Homoleptic α-Metalated *N*,*N*-Dimethylbenzylamine Rare-Earth-Metal Complexes. *Organometallics* **2011**, *30*, 3915–3918. [CrossRef]
81. Bambirra, S.; van Leusen, D.; Meetsma, A.; Hessen, B.; Teuben, J.H. Neutral and cationic yttrium alkyl complexes with linked 1,4,7-triazacyclononane-amide monoanionic ancillary ligands: Synthesis and catalytic ethene polymerization. *Chem. Commun.* **2001**, 637–638. [CrossRef]
82. Bambirra, S.; Boot, S.J.; van Leusen, D.; Meetsma, A.; Hessen, B. Yttrium Alkyl Complexes with Triamido-Amide Ligands. *Organometallics* **2004**, *23*, 1891–1898. [CrossRef]

83. Royal, G.; Dahaoui-Gindrey, V.; Dahaoui, S.; Tabard, A.; Guilard, R.; Pullumbi, P.; Lecomte, C. New Synthesis of *trans*-Disubstituted Cyclam Macrocycles—Elucidation of the Disubstitution Mechanism on the Basis of X-ray Data and Molecular Modeling. *Eur. J. Org. Chem.* **1998**, *1998*, 1971–1975. [CrossRef]
84. Munhá, R.F.; Alves, L.G.; Maulide, N.; Duarte, M.T.; Markó, I.E.; Fryzuk, M.D.; Martins, A.M. *trans*-Disubstituted diamido/diamine cyclam zirconium complexes. *Inorg. Chem. Commun.* **2008**, *11*, 1174–1176. [CrossRef]
85. Hong, S.; Tian, S.; Metz, M.V.; Marks, T.J. C_2-Symmetric Bis(oxazolinato)lanthanide Catalysts for Enantioselective Intramolecular Hydroamination/Cyclization. *J. Am. Chem. Soc.* **2003**, *125*, 14768–14783. [CrossRef] [PubMed]
86. *SAINT*, version 7.03A; Bruker AXS Inc.: Madison, WI, USA, 1997–2003.
87. Sheldrick, G.M. *SADABS, Software for Empirical Absorption Corrections*; University of Göttingen: Göttingen, Germany, 1996.
88. Altomare, A.; Cascarano, G.; Giacovazzo, C.; Guagliardi, A.; Burla, M.C.; Polidori, G.; Camalli, M. SIR92—A program for automic solution of crystal structures by direct methods. *J. Appl. Cryst.* **1994**, *27*, 435.
89. Altomare, A.; Burla, M.C.; Camalli, M.; Cascarano, G.L.; Giacovazzo, C.; Guagliardi, A.; Moliterni, A.G.G.; Polidori, G.; Spagna, R. SIR97: A new tool for crystal structure determination and refinement. *J. Appl. Cryst.* **1999**, *32*, 115–119. [CrossRef]
90. Sheldrick, G.M. Crystal structure refinement with SHELXL. *Acta Cryst.* **2015**, *C71*, 3–8.
91. Farrugia, L.J. *WinGX* and *ORTEP* for Windows: An update. *J. Appl. Cryst.* **2012**, *45*, 849–854. [CrossRef]
92. Spek, A.L. *PLATON SQUEEZE*: A tool for the calculation of the disordered solvent contribution to the calculated structure factors. *Acta Cryst.* **2015**, *C71*, 9–18.
93. Macrae, C.F.; Sovago, I.; Cottrell, S.J.; Galek, P.T.A.; McCabe, P.; Pidcock, E.; Platings, M.; Shields, G.P.; Stevens, J.S.; Towler, M.; et al. *Mercury 4.0*: From visualization to analysis, design and prediction. *J. Appl. Cryst.* **2020**, *53*, 226–235. [CrossRef] [PubMed]
94. Parr, R.G.; Young, W. *Density Functional Theory of Atoms and Molecules*; Oxford University Press: New York, NY, USA, 1989.
95. Frisch, M.J.; Trucks, G.W.; Schlegel, H.B.; Scuseria, G.E.; Robb, M.A.; Cheeseman, J.R.; Scalmani, G.; Barone, V.; Mennucci, B.; Petersson, G.A.; et al. *GAUSSIAN 09 (Revision A.01)*; Gaussian, Inc.: Wallingford, CT, USA, 2009.
96. Zhao, Y.; Truhlar, D.G. The M06 suite of density functionals for main group thermochemistry, thermochemical kinetics, noncovalent interactions, excited states, and transition elements: Two new functionals and systematic testing of four M06-class functionals and 12 other functionals. *Theor. Chem. Acc.* **2008**, *120*, 215–241.
97. Zhao, Y.; Truhlar, D.G. Density Functionals with Broad Applicability in Chemistry. *Theor. Chem. Acc.* **2008**, *41*, 157–167. [CrossRef]
98. Zhao, Y.; Truhlar, D.G. Applications and validations of the Minnesota density functionals. *Chem. Phys. Lett.* **2011**, *502*, 1–13. [CrossRef]
99. Dunning, T.H., Jr.; Hay, P.J. *Modern Theoretical Chemistry*; Plenum Press: New York, NY, USA, 1977; pp. 1–28.
100. Hay, P.J.; Wadt, W.R. Ab initio effective core potentials for molecular calculations. Potentials for the transition metal atoms Sc to Hg. *J. Chem. Phys.* **1985**, *82*, 270–283. [CrossRef]
101. Wadt, W.R.; Hay, P.J. Ab initio effective core potentials for molecular calculations. Potentials for the main group elements Na to Bi. *J. Chem. Phys.* **1985**, *82*, 284–298. [CrossRef]
102. Hay, P.J.; Wadt, W.R. Ab initio effective core potentials for molecular calculations. Potentials for K to Au including the outermost core orbitals. *J. Chem. Phys.* **1985**, *82*, 299–310. [CrossRef]
103. Ehlers, A.W.; Böhme, M.; Dapprich, S.; Gobbi, A.; Höllwarth, A.; Jonas, V.; Köhler, F.; Stegmann, R.; Veldkamp, A.; Frenking, G. A set of f-polarization functions for pseudo-potential basis sets of the transition metals Sc-Cu, Y-Ag and La-Au. *Chem. Phys. Lett.* **1993**, *208*, 111–114. [CrossRef]
104. Ditchfield, R.; Hehre, W.J.; Pople, J.A. Self-Consistent Molecular-Orbital Methods. IX. An Extended Gaussian-Type Basis for Molecular-Orbital Studies of Organic Molecules. *J. Chem. Phys.* **1971**, *54*, 724–728. [CrossRef]
105. Hehre, W.J.; Ditchfield, R.; Pople, J.A. Self-Consistent Molecular Orbital Methods. XII. Further Extensions of Gaussian-Type Basis Sets for Use in Molecular Orbital Studies of Organic Molecules. *J. Chem. Phys.* **1972**, *56*, 2257–2261. [CrossRef]
106. Hariharan, P.C.; Pople, J.A. Accuracy of Ahn equilibrium geometries by single determinant molecular orbital theory. *Mol. Phys.* **1974**, *27*, 209–214. [CrossRef]
107. Gordon, M.S. The isomers of silacyclopropane. *Chem. Phys. Lett.* **1980**, *76*, 163–168. [CrossRef]
108. Hariharan, P.C.; Pople, J.A. The influence of polarization functions on molecular orbital hydrogenation energies. *Theor. Chim. Acta* **1973**, *28*, 213–222. [CrossRef]
109. Wiberg, K.B. Application of the people-santry-segal CNDO method to the cyclopropylcarbinyl and cyclobutyl cation and to bicyclobutane. *Tetrahedron* **1968**, *24*, 1083–1096. [CrossRef]